



The Egyptian International Journal of Engineering Sciences and Technology

Vol. 34 (2021)45–57

<https://eijest.journals.ekb.eg/>



Seismic Evaluation Of RC Buildings

Hamdy K. Shehab Eldin, Hilal Hassan, Heba A. Mohamed and Zainab E. Ragab*

Structural Engineering Department, Zagazig University, Zagazig, Egypt

ARTICLE INFO

Keywords:

Seismic evaluation
Pushover analysis
Inter-story drift
Capacity curve
Seismostruct program.

ABSTRACT

The seismic evaluation of existing buildings is a more troublesome assignment than the seismic design of new buildings. The need for seismic evaluation for buildings becomes necessary to know the level of structural damage and how to cure it due to earthquakes. The seismic evaluation shows how the structure's behavior under seismic loads and determines the ultimate capacity for the structure, there are several methods used in seismic assessment in the analysis which may be static or dynamic. In this study, an educational building located in Egypt has been evaluated for the seismic load to decide if there is a need for retrofitting or not. The seismostruct program is used for modeling and analyzing three dimensional reinforced concrete (RC) buildings with different stories; Ground +4 stories (G+4), Ground +7 stories (G+7), Ground +10 stories (G+10), and Ground +13 stories (G+13) RC building located in different seismic zones; II, III, IV, and zone V. A nonlinear static pushover analysis (POA) using the displacement coefficient method was used to evaluate the seismic performance of the existing building. The analysis results are disseminated in terms of inter-story drift ratio, capacity curves with performance point, and performance criteria checks for each model.

1. Introduction

Recent earthquakes in various parts of the world, as well as the resulting losses, have demonstrated the inadequacy of building structures to carry seismic loads. Seismic evaluation of buildings is required to determine the extent of structural damage and how to repair it as a result of earthquakes. This study aims to define the seismic performance of buildings, based on a Pushover analysis that provides useful data on the building's non-linear behavior. Codes such as ATC-40 [1], FEMA-356 [2], and FEMA-440 [3] have given basic necessity principles rules to perform the nonlinear static pushover analysis. There are several procedures to define the seismic performance

of the building depending on the chosen code, ATC-40 discusses the capacity spectrum method, FEMA-356 suggests the displacement coefficient method, and FEMA 440 describes enhancements to both the capacity spectrum method and the displacement coefficient method. In any case, every one of these procedures requires assurance of nonlinear force-deformation curve, known as "pushover curve" or "capacity curve", that is derived from pushover analysis.

However, the nonlinear dynamic analysis is a theoretically correct approach [4, 5] and is proper for research and significant structure design. But, these days; structural engineers prefer to use pushover analysis as another strategy to solve the expected

* Corresponding author. Tel.: +0201212054347.
E-mail address: eng_zelnagar@yahoo.com

constraints when using dynamic analysis. These constraints are; for any design, the Nonlinear Dynamic Analysis is very complex and not common sense, and it involves time history of knowledge about ground motion and comprehensive structural member hysteretic behavior that is unusual.

Despite the widespread use of the POA in the seismic evaluation of buildings due to its simplicity, due to the inborn limitations in its theory, especially for the assessment of structural collapse capacity checked, the accuracy of this technique still needs to be checked. A variety of studies are done to investigate POA with dynamic analysis in order to check the accuracy and applicability of POA. Twelve RC building models were created to generate the dynamic pushover envelopes and compare them with the static pushover results with different load patterns, the results of more than a hundred inelastic dynamic analyses were used using a comprehensive 2D modeling approach, good correlation is achieved between the measured idealized dynamic analysis envelopes and static pushover outcomes for a given structure class[6]. T. Rossetto, et al. [7] were interested to present a comparative study of various dynamic and static approaches for evaluating building performance under seismic loads and tsunami. It was showed that the proposed double pushover approach produces a reasonable check of the shear forces over the structural elements that are critical to the tsunami response of the structure. For the experimental studies, the accuracy and appropriateness of the POA are investigated by correlation with the dynamic time history analysis (THA) checked by a complete collapse shaking table test ductile RC frame[8]. The obtained comparison results are presented in terms of the top displacement, the inter-story drift ratio, and the curvature of column ends; Such findings have shown that the POA appears to significantly underestimate the structural responses when the structure is severely damaged and near a collapsed state. The errors increase with structural damage improvement, where the most serious error could exceed more than 60 percent. The POA may give wrong judgment on the occurrence of collapse. Reasonable utilization of POA is required while evaluating the structural seismic collapse capacity [8].

One of the broadly studied problems in structural engineering is damage to low, medium, and high-rise RC buildings during seismic tremors. The seismic performance of these buildings during a few past

tremors has been studied by many researchers worldwide. For instance, A. Samanta, and A. Swain [9] had an interest to review “Seismic Response and Vulnerability Assessment of Representative Low, Medium and High-rise Buildings in Patna, India”. The results of this study show that; For low and mid-rise buildings, Peak floor acceleration and average floor acceleration values decrease about 60% and 50%, respectively as compared to fixed base models for low and mid-rise buildings. Where; for high-rise buildings these values increase up to 300% and 50%, respectively as compared to fixed base models. And it is also showing that; for high-rise buildings, the ductility factor is greater than for mid-rise and low-rise buildings. Thus ductility demand may increase for high-rise buildings.

For this study, the studied models are presented in Table 1. This table is arranged in groups to assess the influence of the number of stories; each group is arranged to assess different seismic zone. The studied buildings are modeled and analyzed using the software Seismostruct [10]. These buildings are asymmetrical plan configuration and regular in elevation with 5000mm height for all stories. The obtained results are scattered in terms of inter-story drift, capacity curves with performance point, and performance criteria check for each model.

2. Objectives

The objective of this study is to evaluate through an analytical study, the seismic performance of reinforced concrete (RC) buildings with different stories; (G+4) story to present low rise buildings, (G+7) story to present medium-rise buildings, (G+10) and (G+13) story to present high rise buildings. A nonlinear static pushover analysis using the displacement coefficient method, as described in ATC-40[1], is using to evaluate the seismic performance of the studied RC buildings; The main objectives are as follow:

- To model the studied RC buildings that have been subjected to seismic loading using the SeismoStruct software program.
- To know the impact of stories number on the building performance.
- To know the impact of seismic zone conditions on building performance.
- By knowing the type of failure that is occurred from the seismic action in the weakest members of the building a proper retrofitting should be applied

for the improvement of the seismic behavior of the building.

Table 1: studied models parameters

| | Model ID | Stories | Seismic zone |
|-----------------------------|----------|---------|--------------|
| Group-1- (G+4) Story | (G+4)Z2 | (G+4) | 2(II) |
| | (G+4)Z3 | (G+4) | 3(III) |
| | (G+4)Z4 | (G+4) | 4(IV) |
| | (G+4)Z5 | (G+4) | 5(V) |
| Group-2- (G+7) Story | (G+7)Z2 | (G+7) | 2(II) |
| | (G+7)Z3 | (G+7) | 3(III) |
| | (G+7)Z4 | (G+7) | 4(IV) |
| | (G+7)Z5 | (G+7) | 5(V) |
| Group-3- (G+10) Story | (G+10)Z2 | (G+10) | 2(II) |
| | (G+10)Z3 | (G+10) | 3(III) |
| | (G+10)Z4 | (G+10) | 4(IV) |
| | (G+10)Z5 | (G+10) | 5(V) |
| Group-4- (G+13) Story | (G+13)Z2 | (G+13) | 2(II) |
| | (G+13)Z3 | (G+13) | 3(III) |
| | (G+13)Z4 | (G+13) | 4(IV) |
| | (G+13)Z5 | (G+13) | 5(V) |

3. Seismic evaluation procedure according to ATC-40

The seismic evaluation can be categorized into two groups: (1) global/structural limits and (2) local/component limits [1]. The global limits are the ability to sustain gravity load, lateral load, and lateral deformation. If the ability to sustain gravity load is lost by a component, the building must be able to redistribute the load to other components. The structure system's lateral load resistance does not degrade by more than 20% of the structure's maximum resistance. The lateral deformation of the buildings must be tested against the deformation limits as shown in Table 2. The maximum lateral deformation or the maximum drift is known as the inter-story drift at the target displacement, which is calculated according to equation 1.

$$\delta_t = C_0 C_1 C_2 C_3 S_a \frac{T_e^2}{4\pi^2} \quad (1)$$

where;

δ_t : is known as target displacement or performance point of the building.

C_0 , C_1 , C_2 , and C_3 are modification factors calculated according to ATC-40, [1]

S_a : is that the response spectrum acceleration at the effective fundamental period T_e of the building.

The local/component limits are the element checks (chord rotation capacity and shear capacity). It must be done for all the components of each floor. The deformation capacity of beams and columns controlled by flexure is defined in terms of the total chord rotation capacity; θ as specified in equation 2. The acceptance criteria for plastic hinge rotations of beam and column elements in the RC moment-resistant frame are presented in Tables 3 and Table 4, respectively, as indicated by ATC-40. Therefore, it should be ensured that a member's flexural demand failure and shear failure do not occur before these limits of rotation are reached.

$$\theta = \theta_y + \theta_p \quad (2)$$

where;

θ_y : is the chord rotation capacity at yield.

θ_p : is the plastic part of the chord rotation capacity

Table 2. Lateral deformation limits according to ATC-40;[1]

| Intermediate Occupancy. | Damage Control. | Life Safety. | Structural Stability. |
|-------------------------|-----------------|--------------|-----------------------|
| 0.010 | 0.010-0.020 | 0.020 | 0.33Si/Wi |

4. Methodology followed

- A 3-D model that represents the overall building properties is made using seismostruct program.
- Define the vertical loads.
- Calculate seismic loads.
- Define the lateral loads.
- Define the control node; which is located in the center of mass of the roof floor.
- Define Peak Ground Acceleration (PGA) value.
- Perform pushover analysis.
- The control node displacement is plotted with the base shear to get the capacity curve.
- Check global/structural limits.
- Check local/component limits.

5. Building description

The building under study is an educational reinforced concrete building in Egypt with three X-direction bays and six Y-direction bays, as shown in Fig.1. The number of stories was varied from low-rise through mid-rise to high-rise buildings. The

heights of the stories are 5000 mm for all stories. The bay widths are 8000 mm, 3500 mm for edge and medium bay respectively in X-direction, and the bay width in Y-direction is 5400 mm. The column size varied from (300 x 900) mm for External columns to (300 x 1100) mm for Internal columns and the beam size varied from (300 x 1500) mm for main beams in Y-direction and (300 x 1000) mm for main beams in X-direction to (250 x 600) mm for secondary beams in the Y-direction. All properties (dimension and reinforcement) of building members are presented in Table 5 and illustrated in Fig.2.

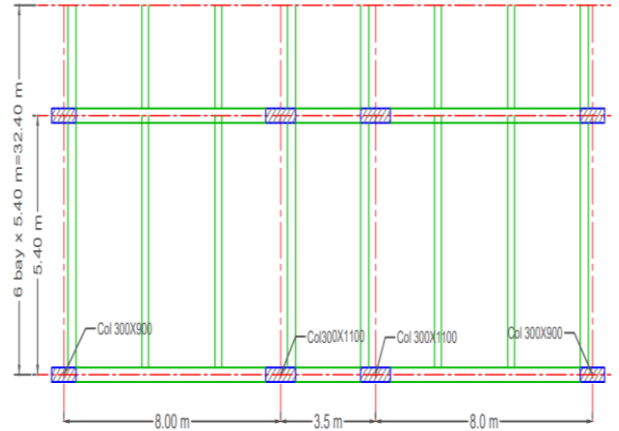


Fig.1. Plan geometry of models.

Table 3. Acceptance Criteria for RC beams controlled by flexure according to ATC-40:[1]

| $\frac{P - P'}{P_{bal}}$ | Trans. Reinf. | $\frac{V}{b_w d \sqrt{f'_c}}$ | Modeling Parameter | | | Plastic Rotation Limit | | |
|--------------------------|---------------|-------------------------------|--------------------------------|------|-------------------------|--------------------------|------------------|---------------------------|
| | | | Plastic Rotation Angle, radian | | Residual Strength Ratio | Performance Level | | |
| | | | a | b | c | Immediate Occupancy (IO) | Life Safety (LS) | Structural Stability (SS) |
| ≤ 0.00 | C | ≤ 3.0 | 0.025 | 0.05 | 0.20 | 0.005 | 0.020 | 0.025 |
| ≤ 0.00 | C | ≥ 6.0 | 0.020 | 0.04 | 0.20 | 0.005 | 0.010 | 0.020 |
| ≥ 0.50 | C | ≤ 3.0 | 0.020 | 0.03 | 0.20 | 0.005 | 0.010 | 0.020 |
| ≥ 0.50 | C | ≥ 6.0 | 0.015 | 0.02 | 0.20 | 0.005 | 0.005 | 0.015 |

Table 4. Acceptance Criteria for RC columns controlled by flexure according to ATC-40:[1]

| $\frac{P - P'}{P_{bal}}$ | Trans. Reinf. | $\frac{V}{b_w d \sqrt{f'_c}}$ | Modeling Parameter. | | | Plastic Rotation Limit | | |
|--------------------------|---------------|-------------------------------|--------------------------------|-------|-------------------------|--------------------------|------------------|---------------------------|
| | | | Plastic Rotation Angle, radian | | Residual Strength Ratio | Performance Level | | |
| | | | a | b | c | Immediate Occupancy (IO) | Life Safety (LS) | Structural Stability (SS) |
| ≤ 0.10 | C | ≤ 3.0 | 0.020 | 0.030 | 0.20 | 0.005 | 0.010 | 0.020 |
| ≤ 0.10 | C | ≥ 6.0 | 0.016 | 0.024 | 0.20 | 0.005 | 0.010 | 0.015 |
| ≥ 0.40 | C | ≤ 3.0 | 0.015 | 0.025 | 0.20 | 0.00 | 0.005 | 0.010 |
| ≥ 0.40 | C | ≥ 6.0 | 0.012 | 0.020 | 0.20 | 0.00 | 0.005 | 0.010 |

Table 5. Properties of building members

| Element | Height (mm) | Width (mm) | Cover (mm) | Long. Reinf. | Trans. Reinf. |
|----------|-------------|------------|------------|-------------------------------|---------------|
| Ext. Col | 900 | 300 | 25 | 16 Ø 16 | Ø8/150mm |
| Int. Col | 1100 | 300 | 25 | 20 Ø 16 | Ø8/150mm |
| MBX | 1000 | 300 | 25 | 9 Ø22 (lower) 4Ø 18 (upper) | Ø8/150mm |
| MBY | 1500 | 300 | 25 | 10 Ø22 (lower) 5Ø 22 (upper)) | Ø8/150mm |

| | | | | | |
|-----|-----|-----|----|-----------------------------|----------|
| SBY | 600 | 250 | 25 | 6 Ø20 (lower) 3Ø 18 (upper) | Ø8/150mm |
|-----|-----|-----|----|-----------------------------|----------|

MBX: Main Beams in X-direction.

MBY: Main Beams in Y-direction.

SBY: Secondary Beams in Y-direction.

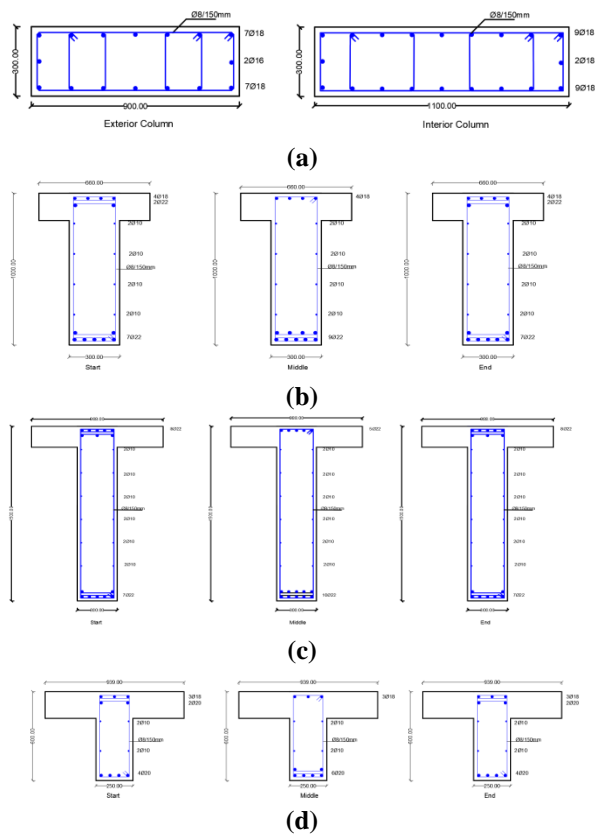


Fig.2. Cross Sections for (a) columns (b) main beams in X-dir (c) Main beams in y-dir and (d) Sec. beams in Y-dir (Dimensions in mm)

6. SeismoStruct Program

Seismostruct Software program is a finite element program, which considers both geometric nonlinearities and material inelasticity. It can also predict, under static or dynamic loading, the large displacement behavior of space frames. The three-dimensional modelling is carried out as shown in Fig.3.

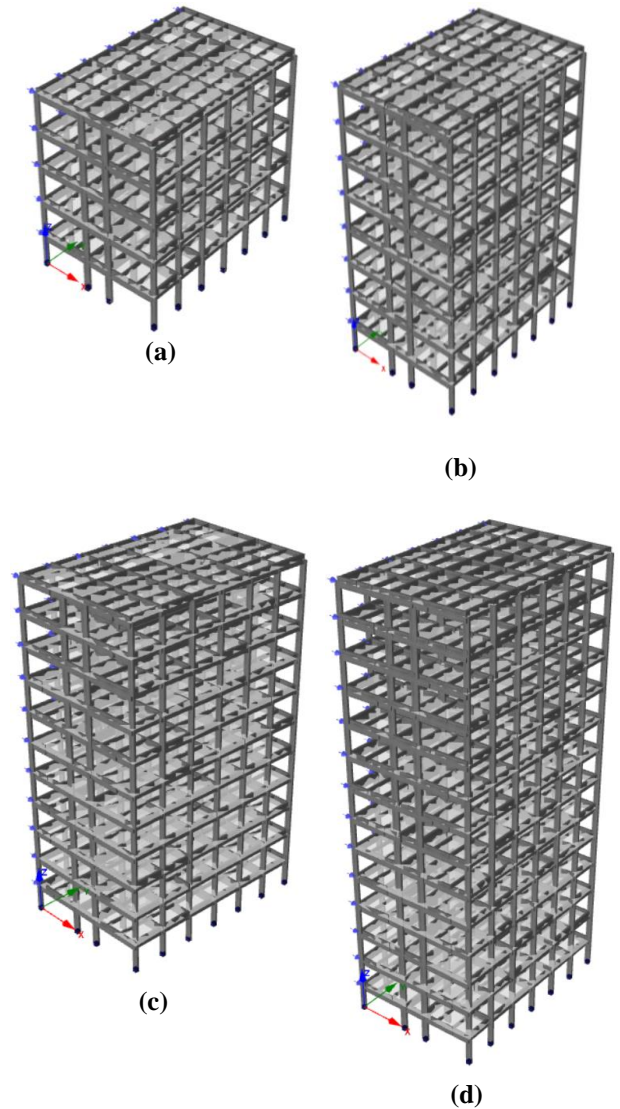


Fig.3. (a) G+4 story building; (b) G+7 story building; (c) G+10 story building; (d) G+13 story building.

6.1. Analytical Models

6.1.1. Material properties

The concrete modeled as (Mander et al. nonlinear concrete model - con_ma) [11]; C16/20 with Confinement factor =1.2; with parameters shown in Table 6. And the reinforcement steel is modeled as (Menegotto-Pint steel model) [12]; S400 with parameters shown in Table 7.

6.1.2. Sections Properties

Beams and columns are modeled as 3D inelastic plastic hinge force-based frame element elements (infrmFBPH) with concentrated inelasticity within a fixed length of the element as proposed by Scott, M.H., and G.L. Fenves [13]. The number of triangular meshes used in section equilibrium computations is set to be 200, 300, 150, and 200 for cross-sections of MBX, MBY, SBY, and columns respectively as shown in Fig.4 and Fig.5. The floor slab of the building possessed very high in-plane stiffness compared to the out-of-plane one; therefore these elements are modeled as 'rigid diaphragm'.

6.1.3. Loads

• Gravity loads

The loads introduced in the software Seismostruct are the dead loads (G) and live loads (Q). Snow loads are very small where the building is located, and they are neglected. The dead loads include the self-weight of the members of the building. The self-weight of the walls has been taken under consideration as a further load (G') within the beams. The external walls that are located in the perimeter of the building have an additional permanent load of 8.00 KN/m that is taken by the perimeter beams. The internal walls have an additional permanent load of 4.00 KN/m taken by the internal main beams. The live loads of the slabs are 4.50 KN/m².

Table 6. Concrete properties

| C16/20 | |
|---------------------------------------|-------|
| Mean compressive strength; (MPa) | 24.0 |
| Modulus of elasticity; (MPa) | 24870 |
| Strain at peak stress | 0.002 |
| Specific weight; (KN/m ³) | 24.00 |

Table 7. Reinforcement properties

| S400 | |
|---------------------------------------|--------|
| Modulus of elasticity; (GPa) | 200.00 |
| Yield strength; (MPa) | 400.00 |
| Strain hardening parameter (-) | 0.005 |
| Fracture/buckling strain (-) | 0.10 |
| Specific weight; (KN/m ³) | 78.00 |

• Lateral loads

According to the Egyptian code of loading; (EPC 201) [14]. The seismic load or base shear force is calculated according to equation 3 and distributed using a triangular load pattern as shown in Fig.6. Then the models are pushed in 100 steps until target displacements are reached or until failure happened.

$$F_{\text{Base_Design}} = \lambda * \left(\frac{W}{g}\right) * S_e(T_1) \quad (3)$$

Where;

λ : is the effective modal mass correction factor.

W: is the seismic weight of the building.

$S_e(T_1)$: is that the ordinate of the designing spectrum at period T_1 .

T_1 : is the fundamental period of vibration of the building for lateral movement in the direction considered.

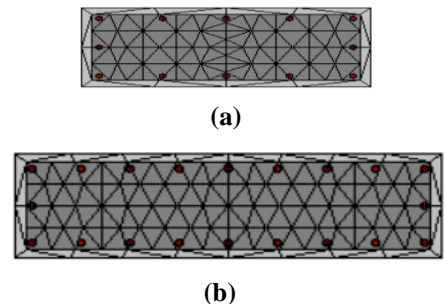


Fig.4. section discretization (triangular meshes); (a) External columns; (b) Internal columns.

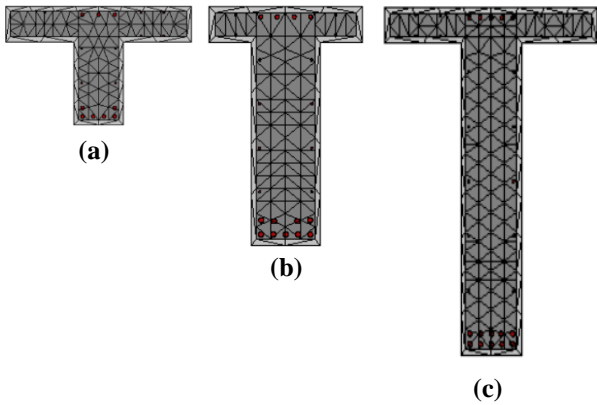


Fig.5. section discretization (triangular meshes); (a) Secondary beams y-dir , (b) Main beams in x-dir & (c) main beams in Y-dir.



Fig.7.Full scale, four-story experimental building; [15]

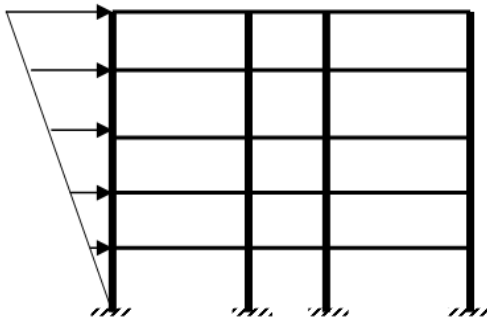


Fig.6. Lateral load triangular distribution.

6.2. Verification

Verification of the model is obtained through comparing results of experimental work with the results of the same model after analyzed it by using seismostruct program to check the validity of the program to simulate the seismic behavior of the RC buildings. The experimental work performed by Sharma, A., et al.,[15]. To simulate a pushover experiment of a full-scale four-story non-seismically detailed RC building shown in Fig.7. Fig.8 displays the overall geometric layout of the tested building indicates that the average beam size was (230 x 1000) mm and the column size ranged from (400 x 900) mm to (300 x 700) mm.

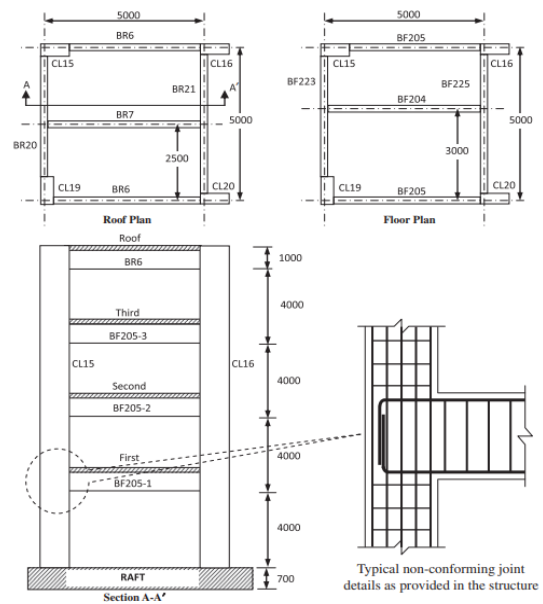


Fig.8. Geometry of the tested building; [15]

After the analysis, the comparison between the experimental and the analytical results from the seismostruct finite element program, in terms of base-shear vs. top displacements, is shown in Fig.9. and in Table 8.

Table 8. The result comparison between the Experimental and the seismostruct-Analytical model

| Displacement (mm) | Experimental Base shear; (KN) | Analytical Base shear; (KN) | Difference (%) |
|-------------------|-------------------------------|-----------------------------|----------------|
| 00.00 | 00.00 | 00.00 | 0.00 |
| 100.00 | 725.00 | 750.00 | 3.448 |
| 200.00 | 840.00 | 900.00 | 7.14 |
| 300.00 | 882.90 | 900.00 | 1.937 |

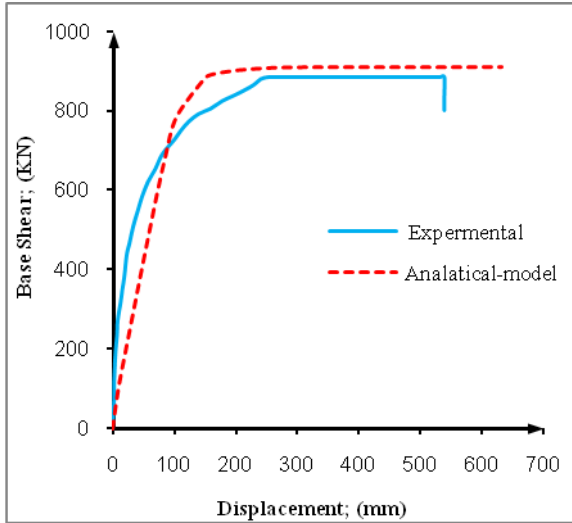


Fig.9. Comparison of Experimental and analytical results.

7. Results and Discussions

Fig.10. shows the pushover curves for studied models with different stories. These curves represent the RC buildings' global behavior with stiffness and ductility. By increasing the number of stories, the slope of pushover curves is gradually reduced. This is because of the progressive development of plastic hinges in the beam and column through the design.

Fig.11. shows the pushover curve with the performance point for each building in different seismic zones according to ATC-40 calculation; as shown in these figures for the same story building; with increasing the seismicity action the performance point of the building increase with the same capacity curve. The building with (G+13) story located in seismic zone V is damaged before reaching its performance point.

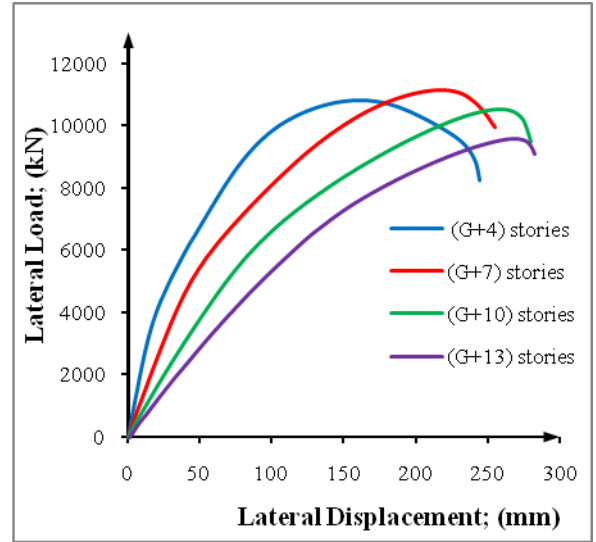


Fig.10. Pushover curve for studied models; (triangular load pattern).

Fig.12.a. shows the inter-story drift ratios for the models with (G+4) story at the calculated performance points. This figure showed that; the maximum inter-story drift ratio occurs in the second story (0.4H) for all (G+4) story models, where H is the overall height of the building. The maximum drift ratio is 0.3%, 0.375%, 0.49%, and 0.6% for building located in seismic zone II,III,IV and V, respectively. This refers to; according to the global evaluation; all (G+4) story buildings can be classified in Immediate Occupancy (IO) performance level as specified in Table 2.

Fig.12.b. shows the inter-story drift ratios for the models with (G+7) story at the calculated performance points. This figure showed that; the maximum inter-story drift ratio occurs in the third story (0.375H) for the first two models and in the second story (0.25H) for the second two models. The maximum drift ratio is 0.285%, 0.35%, 0.49%, and 0.64% for building located in seismic zone II,III,IV and V respectively. This refers to; according to the global evaluation; all (G+7) story buildings can be classified in Immediate Occupancy (IO) performance level as specified in Table 2.

Fig.12.c. shows the inter-story drift ratios for the models with (G+10) story at the calculated performance points. This figure showed that; the

maximum inter-story drift ratio occurs in the fourth story (0.36H) for the first two models and in the third story (0.27H) for the third model located in seismic zone IV and in the first story for the fourth model located in seismic zone V. The maximum drift ratio is 0.31%, 0.38%, 0.5%, and 0.87% for building located in II,III,IV and V, respectively. This refers to; according to the global evaluation; all (G+10) story buildings can be classified in Immediate Occupancy (IO) performance level as specified in Table 2.

Fig.12.d. shows the inter-story drift ratios for the models with (G+13) story at the calculated performance points. This figure showed that; the maximum inter-story drift ratio occurs in the fifth story (0.36H) for the first two models and in the first story for the third model located in seismic zone IV. the maximum drift ratio is 0.34%, 0.405% and 0.71%, for building located in seismic zone II,III and IV, respectively. This refers to; according to the global evaluation; all (G+13) story buildings can be classified in Immediate Occupancy (IO) performance level as specified in Table 2.

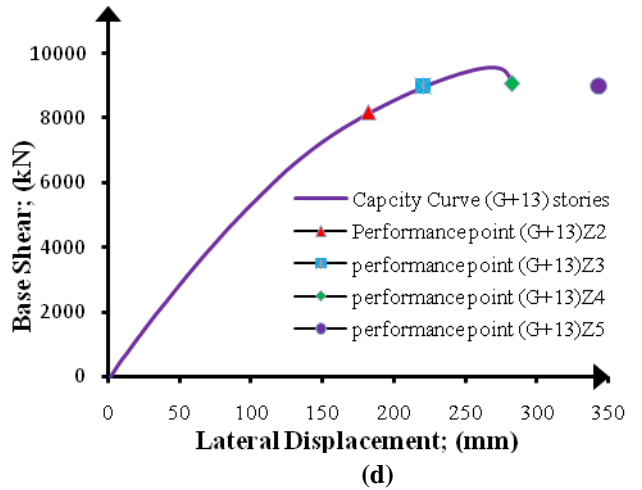
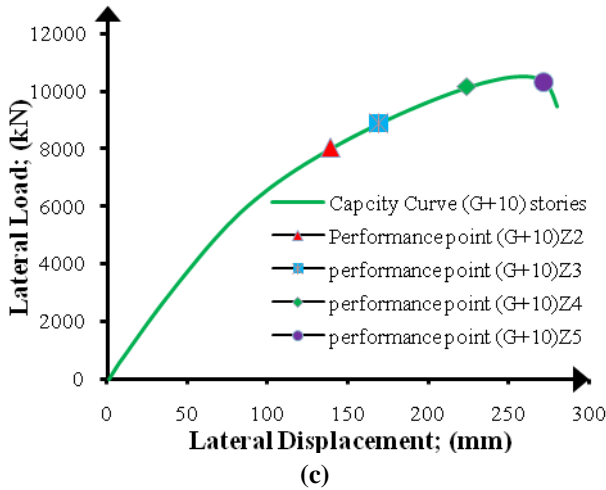
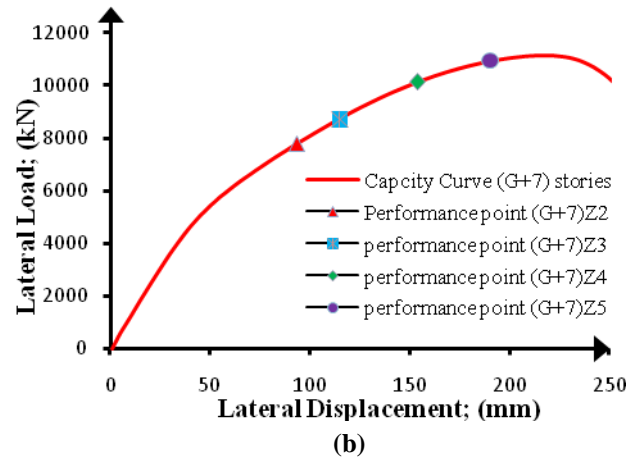
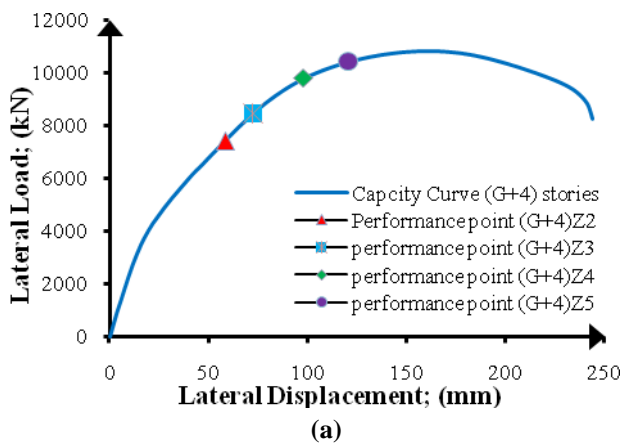


Fig.11. Pushover curve with performance point for: (a) G+4 story building; (b) G+7 story building; (c) G+10 story building; (d) G+13 story building; located in different seismic zones

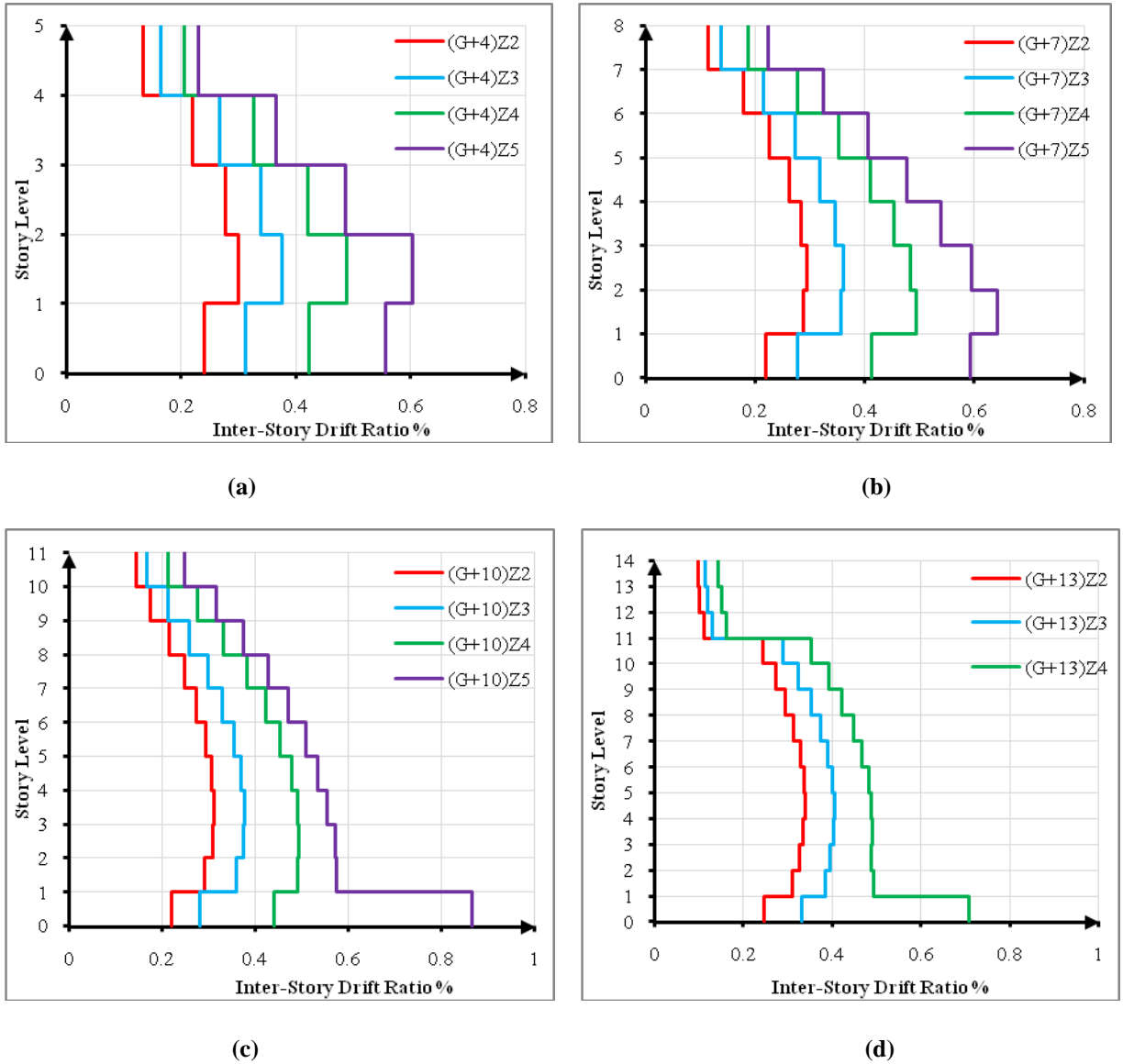


Fig.12. The inter-story drift ratios at performance points: for; (a) G+4 story models; (b) G+7 story models; (c) G+10 story models; (d) G+13 story models; with different seismic zones.

At every analysis step, pushover analysis decides plastic rotation hinge location in the elements and which hinges arrive at ASCE 41-17[16] performance criteria, which are IO (Immediate Occupancy performance level) occurs at yield chord rotation and CP (Collapse Prevention performance level) occurs at chord rotation capacity. The deformed shapes and Plastic hinges formation have been gained at various displacement levels or performance points as shown in Fig.13.

Fig.14. shows the sequence of damage of different stories RC buildings. As shown in these figures the shear capacity of some members is reached very early for all buildings located in different seismic zones; so all RC buildings needed to be retrofitting. The (G+13) story RC building located in seismic zone V; is expected to be a failure before reached its performance point as shown in Fig.14.d.

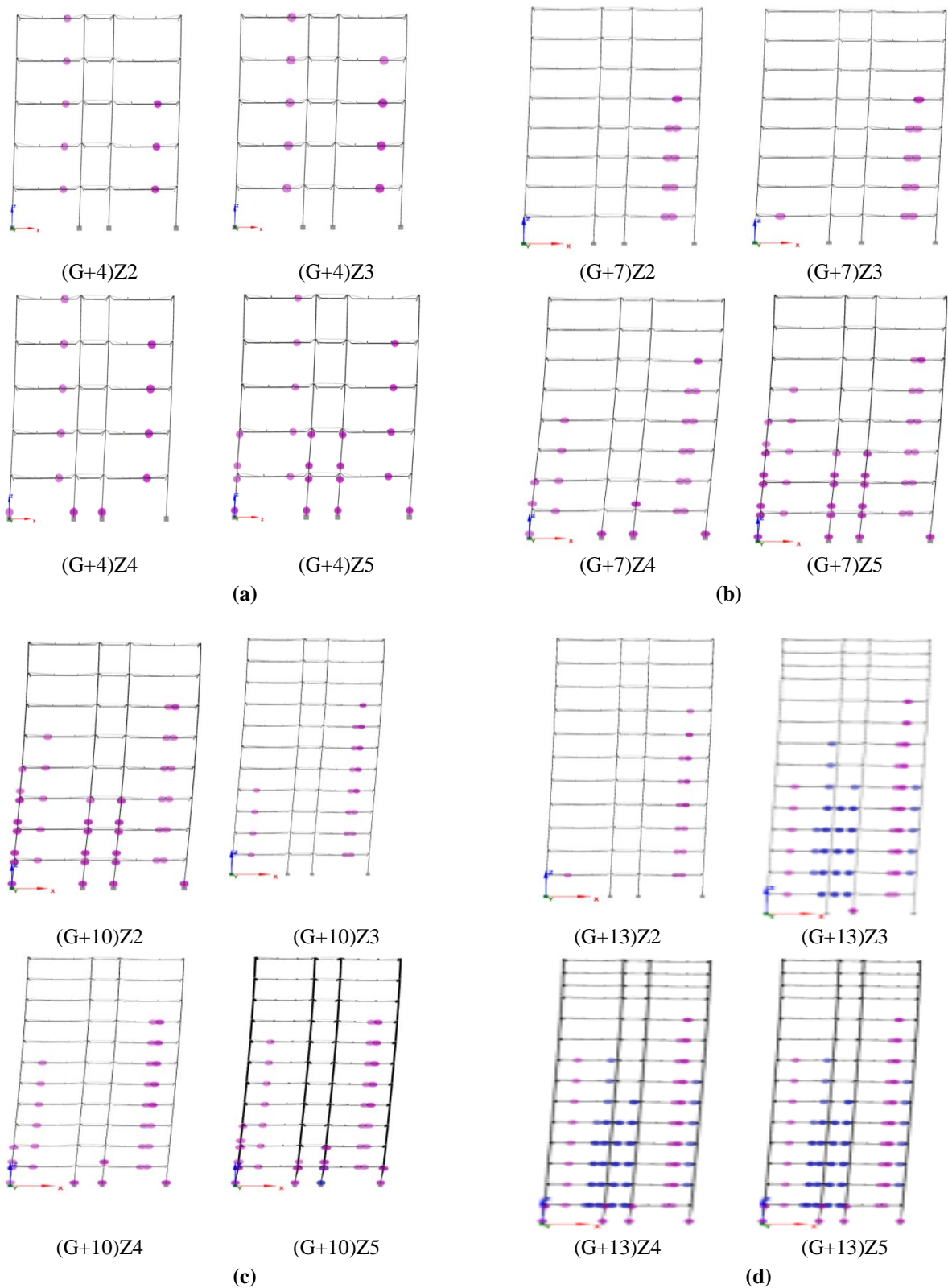
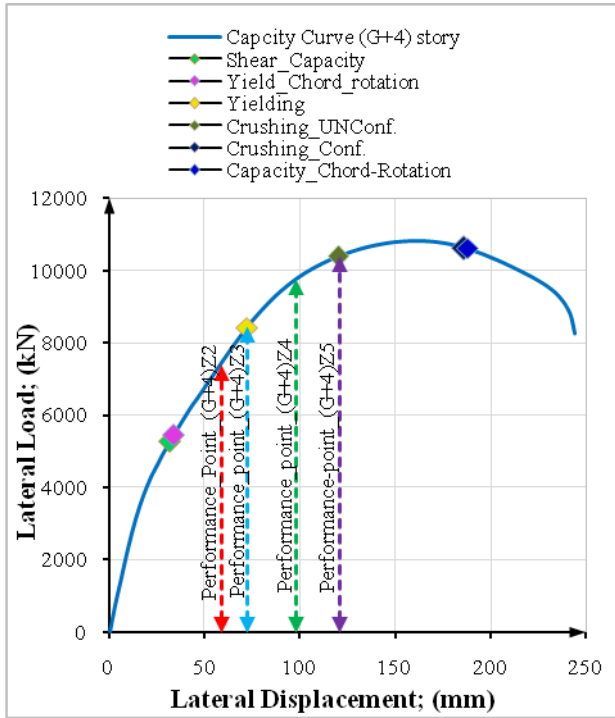
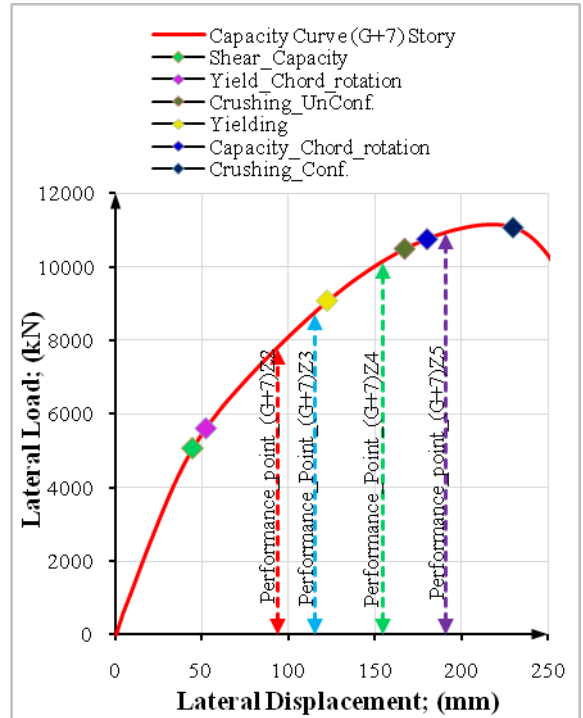


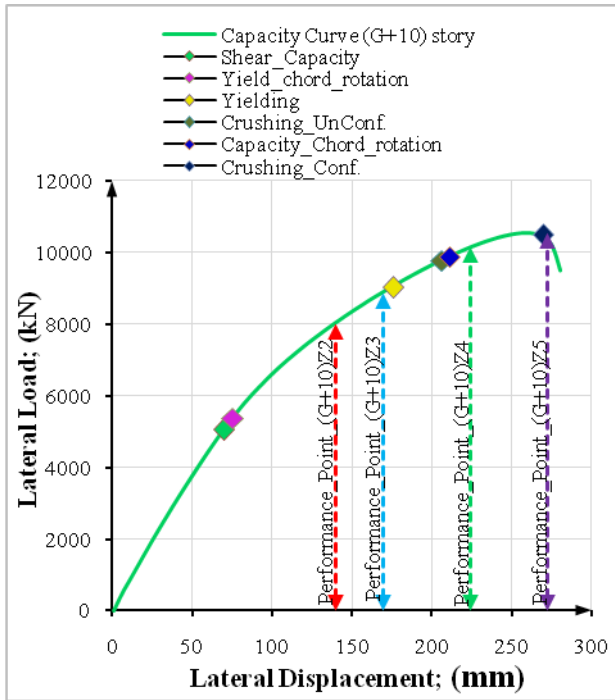
Fig. 13. Plastic hinge formation at the performance point for; (a) G+4 story building; (b) G+7 story building; (c) G+10 story building; (d) G+13 story building; with different seismic zones.



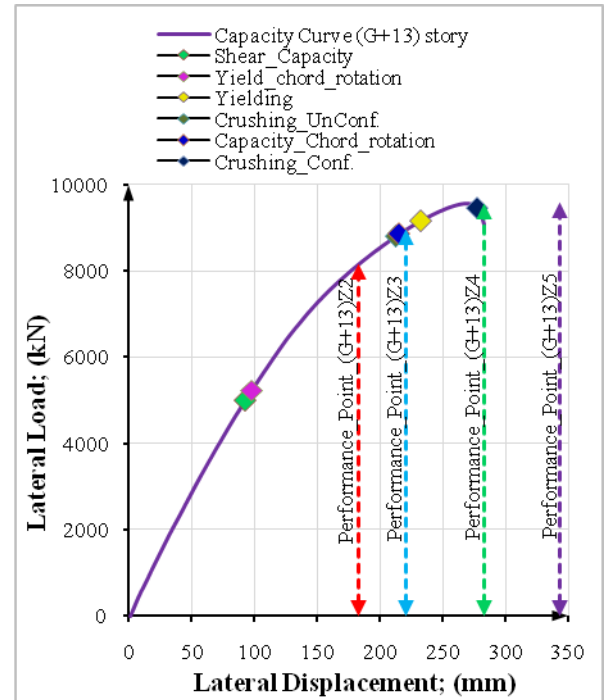
(a)



(b)



(c)



(d)

Fig.14. Sequence of damage: (a) G+4 story building; (b) G+7 story building; (c) G+10 story building; (d) G+13 story building.

8. Conclusions

This study aimed to define the performance of buildings under seismic loads, based on Pushover analysis. The study introduced has considered four groups of RC buildings located in different seismic zones; The first group (G+4) story to present low rise buildings, the second group (G+7) story to present medium-rise buildings, the third group (G+10)story, and the fourth group (G+13) story to present high rise buildings. These buildings are designed based on EPC (201) [14]. The displacement coefficient method as specified in ATC-40 was used to perform the pushover analysis.

The major conclusions of this study are as follows:

1. Pushover analysis is a generally straightforward approach to monitor the nonlinear behavior of the building.
2. For the same building located in different seismic zones; the performance point of the building increases with increasing seismic zone hazards so the inter-story drift ratio increases as well.
3. For the buildings with the same stories, the maximum inter-story drift ratio increase with increasing the seismic zone hazard.
4. According to the global/structural limits; which concerned with the lateral deformation; The maximum inter-story drift ratio for all buildings located in seismic zones II, III, IV and V is expected to be less than 1.0%; this refers to all of these buildings can be classified in Immediate Occupancy (IO) performance level according to ATC-40 specifications.
5. According to local/element limits (chord rotation capacity and shear capacity); it is shown that the shear capacity of some members is reached very early for all buildings located in different seismic zones; so all RC buildings needed to be retrofitting.
6. The global/structural limits are not enough to prove the safety of buildings against lateral loads; local/element limits should be carried out too; as shown in this study the global/structural limits showed the safety of all RC buildings to resist lateral loads but the local/element limits expected that all buildings will be a failure and they are needed to be retrofitting.

References

- [1] ATC-40, "Seismic evaluation and retrofit of concrete buildings," vol. 1, ed. Applied Tecnology Council: Redwood City, CA, 1996.
- [2] "American Society of Civil Engineers," in Prestandard and Commentary for the Seismic Rehabilitation of Buildings, ed. Federal Emergency Management Agency FEMA 356, Washington, D.C., 2000.
- [3] "Applied Technology Council," in Improvement of nonlinear static seismic analysis procedures, ed. Report No. FEMA-440, Washington (DC), 2005.
- [4] R. Suwondo, M. Alama, and S. Ashour, "Seismic Assessment of RC Building According to ATC 40, FEMA 356 and FEMA 440," ARABIAN JOURNAL FOR SCIENCE AND ENGINEERING, vol. 39, pp. 7691-7699, 11/01 2014.
- [5] A. Vijayakumar and D. V. Babu, "Pushover analysis of existing reinforced concrete framed structures," European Journal of Scientific Research, vol. 71, pp. 195-202, 2012.
- [6] A. M. Mwafy and A. S. Elnashai, "Static pushover versus dynamic collapse analysis of RC buildings," Engineering Structures, vol. 23, pp. 407-424, 2001/05/01/ 2001.
- [7] S. Li, Z. Zuo, C. Zhai, and L. Xie, "Comparison of static pushover and dynamic analyses using RC building shaking table experiment," Engineering Structures, vol. 136, pp. 430-440, 2017/04/01/ 2017.
- [8] T. Rossetto, C. De la Barra, C. Petrone, J. C. De la Llera, J. Vásquez, and M. Baiguera, "Comparative assessment of nonlinear static and dynamic methods for analysing building response under sequential earthquake and tsunami," Earthquake Engineering and Structural Dynamics, vol. 48, pp. 867-887, 2019.
- [9] A. Samanta and A. Swain, "Seismic Response and Vulnerability Assessment of Representative Low, Medium and High-rise Buildings in Patna, India," Structures, vol. 19, pp. 110-127, 2019/06/01/ 2019.
- [10] Seissoft, "SeismoStruct – A computer program for static and dynamic nonlinear analysis of framed structures," ed. <http://www.seissoft.com>, 2018a.
- [11] J. B. Mander, M. J. N. Priestley, and R. Park, "Theoretical stress-strain model for confined concrete," Journal of Structural Engineering, vol. 114, pp. 1804-1826, 1998.
- [12] M. Menegotto and P. E. Pinto, "Method of analysis for cyclically loaded R.C. plane frames including changes in geometry and non-elastic behaviour of elements under combined normal force and bending," International Association for Bridge and Structural Engineering, pp. 15-22, 1973.
- [13] M. H. Scott and G. L. Fennes, "Plastic hinge integration methods for force-based beam-column elements," ASCE Journal of Structural Engineering, vol. 132, pp. 244-252, 2006.
- [14] Egyptian Code for Calculation of loads and Forces for Buildings (ECP-201). Research Center for housing and Building, Giza, Egypt, 2012.
- [15] A. Sharma, G. R. Reddy, K. K. Vaze, and R. Eligehausen, "Pushover experiment and analysis of a full scale non-seismically detailed RC structure," Engineering Structures, vol. 46, pp. 218-233, 2013.
- [16] ASCE41-17, "Seismic Evaluation and Retrofit of Existing Buildings," ed: American Society of Civil Engineers, 2017.